Pergamon

Cement and Concrete Research, Vol. 27, No. 10, pp. 1581–1590, 1997

0008-8846/97 $17.00 + .00

PII S0008-8846(97)00161-0

STUDY OF THE STRUCTURAL PROPERTIES OF THE C-S-H(I) BY MOLECULAR DYNAMICS SIMULATION

P. Faucon,*†‡ J.M. Delaye,† J. Virlet,* J.F. Jacquinot‡ and F. Adenot§

*Service de Chimie Moléculaire, C.E.A Saclay, 91191 Gif sur Yvette, France

†Section de Recherche de Métallurgie Physique, C.E.A. Saclay, 91191 Gif sur Yvette, France

‡Service de Physique de l'Etat Condensé, C.E.A. Saclay, 91191 Gif sur Yvette, France

§Service d'Entreposage et de Stockage des Déchets, C.E.A. Saclay, 91191 Gif sur Yvette, France

(Refereed)

(Received December 11, 1996; in final form April 24, 1997)

ABSTRACT

Molecular dynamics have been used for a few years to study glass structures. Hydrogen properties were however difficult to simulate. For the study of cement hydrated structures, this technique has not been used. Calcium silicate hydrates (C-S-H) are the main hydrates of cement pastes. X-ray diffraction has not resolved their structure, but has demonstrated structural similarities with tobermorite. ^{29}Si magic-angle spinning nuclear magnetic resonance spectroscopy has revealed that as the Ca/Si molar ratio in the C-S-H is increased breaks occur in the chains of silicon tetrahedra, which are of infinite length in tobermorite. Molecular dynamics simulation gives atomic-level information. It complements Si-NMR, which does not give the full structure. It has been possible to simulate the partially covalent properties of the hydrogen and silicon bonds using pair and three-body potentials. Relaxation of the tobermorite structure (Ca/Si = 0.66 and 0.83) with 2500 atoms was studied in order to identify the sources of structural instability and to understand the breaking mechanisms in the C-S-H chains. The effects of cationic substitutions on the structure of tobermorite have been studied. Aluminum preferentially substitutes for the bridging silicon of the structure. The charge deficit introduced by the substitution is compensated by protons. Regardless of the substitution site, the aluminum is always flanked by two tetrahedrally coordinated silicon atoms. Calcium ions move to the substituted sites and complete the charge compensation of the protons. © *1997 Elsevier Science Ltd*

Introduction

Calcium silicate hydrates (C-S-H) are the main components of hydrated cements. They are characterized by an X-ray diffraction pattern with few peaks (1). Without being amorphous, they have a structure organized over distances of less than 100 Å. X-ray diffraction has not resolved their structure, but has demonstrated structural similarities with tobermorite. These

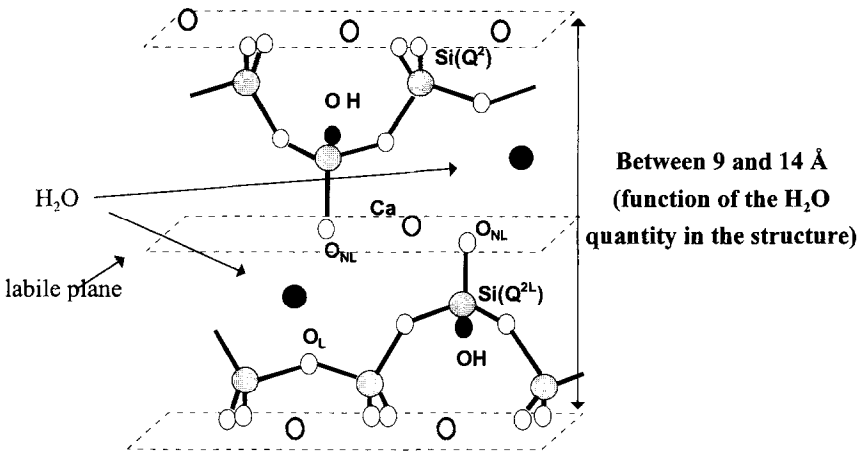

FIG. 1.
Nonsubstituted tobermorite.

similarities have also been established by ^{29}Si magic-angle spinning nuclear magnetic resonance spectroscopy (MAS-NMR) (2–8).

C-S-H have a variable stoichiometry (1–9), and are commonly defined by their Ca/Si ratio. In this study, we focused solely on C-S-H(I) of Ca/Si ratios 0.66 and 0.83. C-S-H(I) have lower Ca/Si ratios than in commercial concrete, where the Ca/Si ratios are about 1.6–1.7. Their structures are the closest to that of 11-Å tobermorite and present better properties for nuclear applications (10–11).

The composition of tobermorite is $Ca_{4+x}Si_6O_{14+2x}(OH)_{4-2x}(H_2O)_2$, generally with $0 \leq x \leq 1$. Tobermorite has infinite chains of silicon tetrahedra that run between layers of calcium atoms (Fig. 1). One calcium layer in three is "labile," i.e., the calcium atoms are statistically distributed among the sites. At a Ca/Si ratio of 0.66, the labile layers are empty (12). As the Ca/Si ratio increases, the labile layer is progressively occupied. The maximum occupancy observed in natural nonsubstituted tobermorites is 50% for Ca/Si = 0.83 (12). For Ca/Si = 0.66, the nonbridging oxygens (O_{NL} in Fig. 1) of the bridging tetrahedra (Q^{2L}) are hydroxylated. The incorporation of labile calcium atoms in the structure creates an excess positive charge, which is compensated by the loss of the protons of these oxygens (12).

For Ca/Si = 0.66, the various models postulated for the structure of the C-S-H(I) agree to describe the structure on the basis of infinite silicon chains as in the tobermorite with similar Ca/Si (7,9,13). These models are validated by the ^{29}Si-MAS-NMR results (2–8). ^{29}Si-MAS-NMR revealed that as the Ca/Si molar ratio in the C-S-H(I) is increased, silicon tetrahedra connected only with one silicate tetrahedron (Q^1) appear in the structure. For Ca/Si about 0.8, Grutzeck et al. (2), Okada et al. (3), and Klur (8) observed a Q^1 percentage between 10% and 20%. This presence of Q^1 in the ^{29}Si-MAS-NMR spectrum is not taken into account in the classical models when the Ca/Si ratio is lower than 0.85 in the C-S-H. For higher Ca/Si > 1, (C-S-HII) ^{29}Si-MAS-NMR clearly demonstrate that the Q^1 tetrahedra results of the omission of silicate tetrahedra in the silicate lattice (8). However, for the C-S-H(I), ^{29}Si-MAS-NMR sensibility is not sufficient to clarify if the Q^1 are resulting from a chain fission or from an omission of silicate tetrahedra.

Numerous cationic substitutions can be made in the tobermorite structure. In particular,

Al^{3+} can substitute for Si^{4+} at the tetrahedral sites. Hydration of slag cements, for example, is characterized by the incorporation of aluminum in the C-S-H structure (14). These silicate-rich cements contain C-S-H of a Ca/Si ratio close to that of tobermorite. Peak ratios in ^{29}Si-MAS-NMR spectroscopy indicate that aluminum is incorporated in a bridging position in the chains of tetrahedrally coordinated silicon.

NMR provides information on the environment of the silicon, but does not give the full structure. Molecular dynamics simulation gives atomic-level information that complements NMR data. We studied the relaxation of the tobermorite structure for Ca/Si = 0.66 and 0.83 in order to identify the sources of structural instability and to understand the mechanisms causing breaks in the C-S-H(I) chains. Those results were also used to investigate the relaxation of substituted tobermorite in order to clarify the mechanisms of incorporation of aluminum into tobermorite structure.

Computational Procedures

Our objective in this work is to study the molecular dynamic of the C-S-H(I) with a tobermorite structure for different Ca/Si and various types of silicon substitutions by aluminum. Monte-Carlo calculations (Energy Minimization) can not reproduce bond changes, dynamics in a structure, and especially the fundamental reaction that can occur in hydrates:

$$\text{Si-O-Si} + H_2O \rightarrow 2\ \text{Si-OH}$$

We had the choice between empirical potentials or quantum potentials to simulate the interactions between the atoms. Because of the small systems necessary for quantum calculations, we have chosen to use empirical potentials to be able to reproduce the crystallographic lattice of the tobermorite.

Born–Mayer–Huggins types of atomic interaction potentials were used to simulate the interaction between two atoms (15). The potential energy of a pair of atoms (i,j) separated by a distance r_{ij} equals:

$$\phi(r_{ij}) = A_{ij}\exp(-r_{ij}/\rho_{ij}) + [q_iq_j/(4\pi\varepsilon_0 r_{ij})]\text{erfc}\ (r_{ij}/\alpha) \quad (1)$$

The first term of this equation corresponds to a repulsion and the second to a Coulombic interaction. To minimize calculation time, the Ewald summation in reciprocal space was neglected. The terms q_i and q_j represent formal charges of the atoms i and j; α was taken as 7 Å.

Five types of atoms are included in the calculations: Si, O, H, Ca, and Al. The values of A_{ij} and ρ_{ij} are given in Table 1.

We used the potentials of Stillinger and Rahman (16) in the representation of the water molecules. These potentials allow dissociation of a water molecule into an OH^- ion and an H^+ proton (17). Pair potentials were applied to the atom pairs Si-H, H-H and O-H:

$$\phi(rij) = a_{ij}/[1 + \exp(b_{ij}/(r_{ij} - c_{ij}))] \quad (2)$$

Table 2 gives values for a_{ij}, b_{ij} and c_{ij}. A single term of the form of Eq. 2 is applied to Si-H interactions, two terms are applied to H-H interactions, and three to O-H interactions.

Three-body potentials were applied to the angles Si-O-H and H-O-H to improve the representation of the local angles (17). These potentials have the following form:

$$\phi(r_{ij},r_{ik},\theta_{jik}) = \lambda_i\exp[\gamma_i/(r_{ij} - r_{ci}) + \gamma_i/(r_{ik} - r_{ci})](\cos\theta_{jik} - \cos\theta_0)^2 \quad (3)$$

TABLE 1
Parameters for two-body potentials

	A_{ij} (10^{-9} erg)	ρ_{ij} (Å)
Si-Si	1.877	0.29
Al-Al	3.418	0.29
Ca-Ca	27,373	0.29
H-H	0.034	0.35
O-O	0.725	0.29
Si-O	2.962	0.29
Al-O	2.750	0.29
Ca-O	10.5104	0.29
O-H	0.3984	0.29
Si-H	0.069	0.29
Si-Ca	7.2	0.29

This equation imposes a constraint on the local angle θ_{jik} of the triplet (j,i,k) to bring it close to the angle θ_0. λ_i and γ_i are adjustable parameters (Table 3). Three-body potentials such as those of Eq. 3 were also applied to the triplets O-Si-O and Si-O-Si.

Site energy is taken here as the energy of an atom occupying the site, i.e., the energy of an atom at a given site is equal to the half-total of the pair energies formed by this atom with its neighbors. For three-body interactions, the energy of the triplet (j,i,k) is wholly attributed to the central atom. The proportion of energy from the three-body potentials is low compared with that from two-body potentials.

The atomic positions in the initial cell are those proposed by Hamid for 11-Å tobermorite (12). Two MD simulations without aluminum, at Ca/Si = 0.66 (cell 1) and Ca/Si = 0.83 (cell 2), were made (Table 4) to study the effect of calcium introduction in the labile plane.

In simulations 3 and 4 (Table 4), 2 of 6 silicons of cell 2 (Ca/Si = 0.83) are substituted by aluminum. Our objective was to test one of the possible balancing charge mechanisms for the Si substitution by Al in the C-S-H. We have chosen to work on Al-substituted structures with Ca/(Si+Al) ratios of 0.83 to compare them with the nonsubstituted structure with a Ca/Si ratio of 0.83 (cell 2). The *global* neutrality is then conserved in the Al-substituted structure by the introduction of protons in the lattice: $Si^{4+} \rightarrow Al^{3+} + H^{+}$. The case of a charge compensation by additional calcium ions in the structure is not considered. The objective of simulations 3 and 4 is then to study the *local* mechanisms of charge balancing

TABLE 2
Parameters for additional water potentials

	a_{ij} (10^{-11} erg)	b_{ij} (Å)	c_{ij} (Å)
Si-H	−4.6542	6.0	2.2
H-H	−5.2793	6.0	1.51
	0.3473	2.0	2.42
O-H	−2.0840	15.0	1.05
	7.6412	3.2	1.50
	−0.8336	5.0	2.0

TABLE 3
Parameters for three-body potentials

	λ (10^{-11} erg)	γ (Å)	r_0 (Å)	θ_0
O-Si-O	19.0	$\gamma_{Si-O} = 2.8$	3.0	109.5°
O-Al-O	19.0	$\gamma_{Al-O} = 2.8$	3.0	109.5°
Si-O-Si, Al-O-Si, Al-O-Al	0.3	$\gamma_{O-Si} = 2.0$	2.6	109.5°
Si-O-H	5.0	$\gamma_{O-Si} = 2.0$	$r_{O-Si} = 2.6$	109.5
		$\gamma_{O-H} = 1.2$	$r_{O-H} = 1.5$	
H-O-H	35.0	1.3	1.6	104.5

in the Al-substituted structure around the aluminum tetrahedra and to determine their structural effects.

When Ca/Si = 0.83, the two Q^{2L} tetrahedra of the cell each have one nonprotonated oxygen O_{NL}. The charge deficit created by the introduction of aluminum into the structure $Si^{4+} \leftrightarrow Al^{3+}$ is therefore compensated by the introduction of protons to the two nonbridging, nonprotonated oxygens of the cell: $O_{NL} \rightarrow OH_{NL}$. All the nonbridging oxygens are therefore hydroxylated. The hydrogens are randomly situated about 1 Å from the oxygens. Two cases are considered: two aluminum atoms substituting for the bridging silicons (simulation 3), and one in a bridging site and the other in a nonbridging site (simulation 4). In both simulations, 50% of the Ca sites in the labile planes are occupied.

The parallelepiped simulation cell contains a whole number of orthorhombic cells of tobermorite, and is repeated to infinity by periodic conditions.

The presence of hydrogen atoms (mass 16 times less than that of oxygen) imposes a 10^{-16} s time step for the MD simulations (10^{-15} s in glasses (17)). The simulations were done for cells of more than 2000 atoms, reproducing the initial cell 16-fold.

The calculations were performed with a constant-volume algorithm, and the successive positions of the atoms were determined by the classical equations of Verlet. The use of formal charges necessitated adjustment of the cell volume. If this adjustment is not made, the electrostatic interactions, in particular with the hydrogens, are too strong and destabilize the structure. With this adjustment, Garofalini's et al. work on the silica gel precipitation (17) demonstrates that the potentials used in this paper are especially good to follow the evolution of a silica lattice in the presence of water. Moreover, with similar potentials Delaye and Ghaleb (19) were able to reproduce irradiation cascade on a glass structure with seven types of atoms in a cell of 200,000 atoms. To have a good structure prediction, the molecular

TABLE 4
Compositions of the different simulation cells

	Initial position of Al^{3+}	$O_{NL}H$	Occupancy of calcium atoms in labile planes	Total number of atoms
Cell 1	No substitution	100%	0%	2432
Cell 2	No substitution	50%	50%	2368
Cell 3	100% of Si (Q^{2L}) substituted	100%	50%	2496
Cell 4	50% of Si (Q^{2L}) substituted 50% of Si (Q^2) substituted	100%	50%	2496

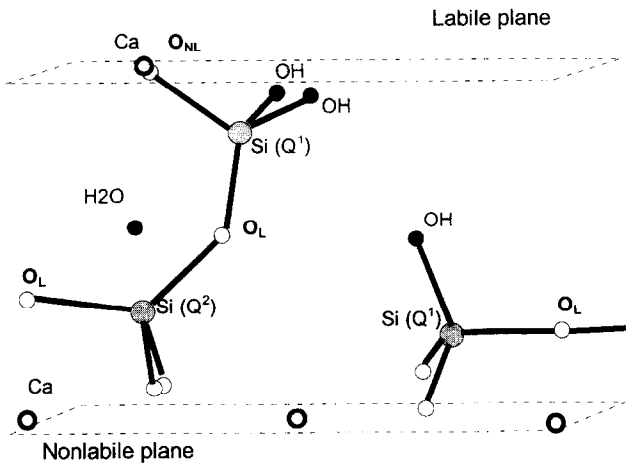

FIG. 2.
Rupture in nonsubstituted tobermorite (Ca/Si = 0.83).

dynamic of the tobermorite structure was studied in function of its density (18). In order to reproduce the Hamid's structure for a Ca/Si = 0.66, the unit cell was therefore expanded by 10% along each axis (yielding a density of 1.8 g/cm^3).

Before each simulation, a 1500-step quenching sequence rapidly moved each type of ion along the lines of force it experiences to the nearest equilibrium site. This technique allowed initial adjustment of the position of the H^+ ions in the H_2O molecules.

The relaxations were done at 800 K. Relaxations at lower temperatures showed that the final structures had not reached their equilibrium structure after 10 ps (18).

Results and Discussion

A preliminary study of the coordination of silicon and aluminum, and of the Si-O and Al-O distances in the relaxed structures, showed that silicon and aluminum were always tetrahedrally coordinated, with mean Si-O and Al-O distances of 0.16 nm and 0.18 nm, respectively. The mean O-H distances were always approximately 0.1 nm. The distributions of the H-O-H and Si-O-H angles were centered on respective values of 104.5° and 109.5°. The three-body potentials therefore allow reproduction of well defined local angular order when the bonds are strongly covalent.

Nonsubstituted Structures

Relaxation of the Ca/Si = 0.66 structure at 800 K did not result in rupture of the chains (18).

The substitution $2H^+ \rightarrow Ca^{2+}$ labile (Ca/Si = 0.83) leads to the formation of about 15% of end-chain Q^1 tetrahedra (Fig. 2), and the Si-Ca distance is then much shorter than with Ca/Si = 0.66 (Fig. 3).

For Ca/Si = 0.66, the O_{NL} oxygens of the bridging tetrahedra (Fig. 1) are hydroxylated. The compensation of charges around the O_{NL} is then assured. At Ca/Si = 0.83, the substitution $2H^+ \rightarrow Ca^{2+}$ labile creates a charge deficit on the oxygens of the bridging

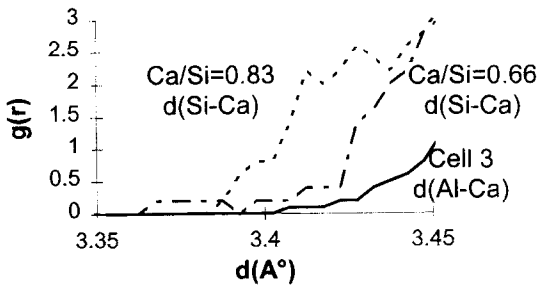

FIG. 3.
Distribution of the Si-Ca distance after relaxation at 800 K.

tetrahedra. This compensation is only possible through the partial rupture of the chains of tetrahedrally coordinated silicon, which allows the distance O_{NL}-Ca to be reduced. O_{NL} is part of the tetrahedral coordination of silicon, and the distance Si-Ca is therefore also reduced. The rupture involves the tetrahedra of sites $Si(Q^2)$ and $Si(Q^{2L})$, via dissociation of a H_2O molecule. The two hydrogens provided by the water explain why the two nonbridging oxygens created by the dissociation are hydroxylated. The mechanism is therefore as follows:

$$Si(Q^{2L})\text{-}O\text{-}Si(Q^2) + H_2O \rightarrow Si(Q^{2L})\text{-}OH + Si(Q^2)\text{-}OH$$

Aluminum at Bridging Sites

Relaxation of cell 3 at 800 K does not rupture the chains, unlike relaxation without substitution for Ca/Si = 0.83. Before MD simulation, the substitution $Si^{4+}{}_{bridging} \rightarrow Al^{3+}{}_{bridging} + H^{+}{}_{NL}$ compensates the charge deficit of the O_{NL} oxygens of the bridging tetrahedra existing for Ca/Si = 0.83. Labile calcium therefore has no role to play. H^+ and Ca^{2+} are first neighbors and so repel one another. MD therefore results in a lengthening of the Al-Ca distance (Fig. 3). No chain rupture is observed.

Aluminum in Bridging and Nonbridging Sites

Two types of substitution occur in cell 4:

$$\text{Type 1: } Si^{4+}(Q^{2L}) \rightarrow Al^{3+}(Q^{2L}) + H^+$$

$$\text{Type 2: } Si^{4+}(Q^2) \rightarrow Al^{3+}(Q^2) + H^+$$

Before MD, the H^+ are linked to the O_{NL} oxygens of the bridging tetrahedra (Q^{2L}). In the case of type 2 substitution, the protons theoretically compensating the charge deficit are relatively distant from the aluminum atoms. Charge compensation is therefore poor. After MD, the protons still compensate poorly for the charge deficit created by the substitution of Si^{4+} by Al^{3+} in cell 4 (Fig. 4). In the presence of nonbridging aluminum, calcium contributes to charge compensation (Fig. 5). The Al-Ca distance in cell 4 is shorter than in cell 3.

After MD simulation, there are occasional ruptures in the chains of tetrahedra. Figure 6

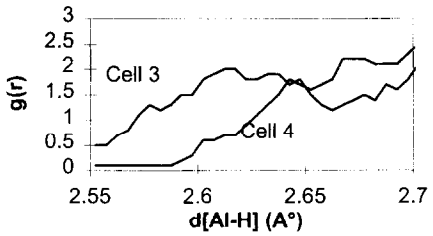

FIG. 4.
Distribution of the Al-H distances after relaxation in cells 3 and 4.

shows that the poor charge compensation of the $Al(Q^2)$ can result in rupture of the chains between two silicon tetrahedra:

$$Si(Q^{2L})\text{-}O\text{-}Si(Q^{2L}) + H_2O \rightarrow 2Si(Q^1)\text{-}OH$$

This rupture allows the formation of a Q^1 tetrahedron in which three of the four oxygens of the tetrahedral coordination are protonated. The position of the $Si(Q^1)$ tetrahedron is a function of the attraction exerted by the $Al(Q^2)$ tetrahedron, which is not charge compensated, on the protons associated with the $Si(Q^1)$ tetrahedron. The same phenomenon is seen with the $Al(Q^{2L})$ tetrahedron, the tilting of which with respect to its presimulation position allows its OH groups to "share" their protons with the $Al(Q^2)$ tetrahedra.

However, the compensation is less effective than in cell 3 (Fig. 4), where the oxygens of the sphere of coordination of the aluminum atoms are themselves protonated. The calcium atoms therefore also participate in the compensation (Fig. 5). In the nonlabile plane, chain rupture allows the coming together of $Al(Q^2)$ and Ca nonlabile. In the labile plane, sharing of the protons of the $Al(Q^{2L})$ with the $Al(Q^2)$ prevents the $Al(Q^2)$ from adequately compensating the charge deficit of the substitution of Al^{3+} for Si^{4+}. Labile calcium therefore also participates in this compensation.

The protons retain their fundamental role in charge compensation. This role is facilitated because protons are small and light and therefore move rapidly. However, sharing of the protons between different sites lacking positive charges is inadequate, so the calcium atoms complete charge compensation by the protons. The structural reorganization induced by MD results in the formation of a limited number of $Si(Q^1)$ tetrahedra. In accordance with the NMR results, no end-chain aluminum is observed (20).

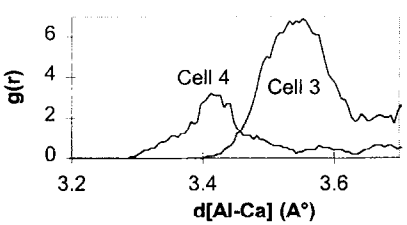

FIG. 5.
Distribution of the Al-Ca distances after relaxation in cells 3 and 4.

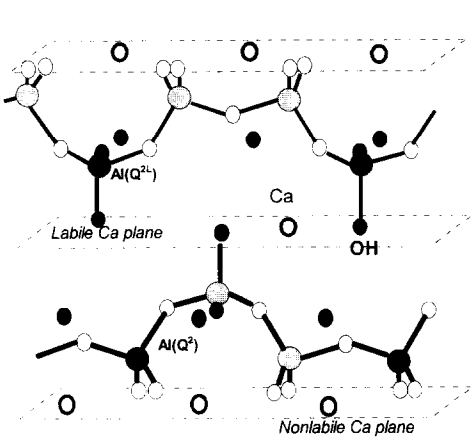

Before MD simulation

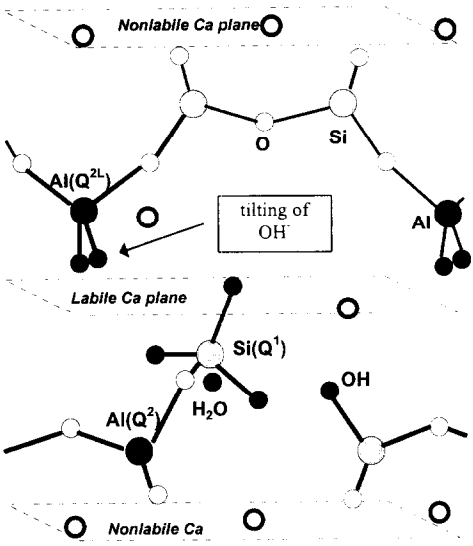

After MD simulation
(Not at the same scale as before MD: The lattice parameters are the same before and after MD)

FIG. 6.
Aluminum in bridging and nonbridging sites: the chain rupture.

Conclusions

Molecular dynamics simulation aids understanding of NMR data concerning C-S-H with $0.66 < Ca/Si < 0.83$. The structure of tobermorite has long served as a model for this type of C-S-H. In the absence of labile calcium atoms, no break in the chains is observed. The substitution $2H^+ \rightarrow Ca^{2+}{}_{labile}$ causes a partial rupture in the chains of tetrahedrally coordinated silicon between bridging silicon (Q^{2L}) and nonbridging silicon (Q^2). This rupture is explained by the formation of $Si(Q^{2L})$-O-Ca_{labile} bonds, which replace the Si-OH bonds. The break occurs via a water molecule, which dissociates, thereby enabling four-coordination to be preserved for each tetrahedron. The hydrogens released by the dissociation allow the formation of two new OH bonds with the two Q^1 tetrahedra.

Substitution of Si^{4+} by Al^{3+} may also occur. Substitution of bridging silicon, which is energetically less stable than nonbridging silicon, is therefore the most favored. Charge deficit is then compensated mainly by protons. In the case of substitution of bridging tetrahedra, the relaxation results in no chain breaks, because the protons are associated with the oxygens of the tetrahedrally coordinated aluminum. When nonbridging silicons are substituted (unfavourable case), the compensation protons are not carried by the oxygens of the tetrahedrally coordinated aluminum. The chains then break and Q^1 tetrahedra are formed. The structural reorganization allows the protons to move towards the aluminum atoms to compensate the charge deficit caused by the substitution of Al^{3+} for Si^{4+}. The calcium atoms also play this role. Despite the observed structural reorganization, each aluminum tetrahedron is systematically coordinated to two silicon tetrahedra, as indicated by NMR (21).

Acknowledgments

We express particular thanks to M. Nonat, of the Laboratoire de Réactivité des Solides at the University of Dijon for helpful discussions about the structure of the C-S-H. We are also grateful to the Agence Nationale pour les Dechets Radioactifs (ANDRA) for cofinancing this study with the CEA.

References

1. H.F.W Taylor, J. Chem. Soc. 33, 163 (1953).
2. M. Grutzeck, A. Benesi, and B. Fanning, J. Am. Ceram. Soc. 72, 665 (1989)
3. Y. Okada, H. Ishida, and T. Mitsuda, J. Am. Ceram. Soc. 77, 765 (1994).
4. X. Cong and R. J .Kirkpatrick, Adv. Cem. Res. 27, 103 (1995).
5. A.R. Brough, C.M. Dobson, I.G. Richardson, and G.W. Groves, J. Am. Ceram. Soc. 77, 593 (1994).
6. A.R. Brough, C.M. Dobson, I.G. Richardson, and G.W. Groves, J. Mater. Sci. 29, 3926 (1994).
7. A. Nonat and X. Lecoq, Proc. of. 2nd Int. Conf. NMR on Cement-Based Materials, Bergamo, 1996, Springer-Verlag (in press).
8. I. Klur, PhD Thesis Université, Paris VI (1996).
9. H.F.W. Taylor, J. Am. Ceram. Soc. 69, 464 (1986).
10. P. Faucon, C. Richet, C. Lefebvre, F. Adenot, J.F. Jacquinot, and J.C. Petit, Proc. 5th Conference of the European Ceramic Society, Versailles (1997).
11. P. Faucon, PhD Thesis, Cergy-Pontoise (1997).
12. S.A Hamid, Zeit. Kristallogr. 154, 189 (1981).
13. I.G. Richardson and G.W. Groves, Cem. Concr. Res. 22, 1001 (1992).
14. I.G. Richardson, A.R. Brough, R. Brydson, G.W. Groves, and C.M. Dobson, J. Am. Ceram. Soc. 76, 2285 (1993).
15. T.F. Soules, J. Chem. Phys. 71, 570 (1979).
16. F.H. Stillinger and A. Rahman, J. Chem. Phys. 68, 666 (1978).
17. B.P. Feuston and S.H. Garofalini, J. Phys. Chem. 94, 351 (1990).
18. P. Faucon, J.M. Delaye, and J. Virlet, J. Sol. State. Chem. 127, 92 (1996).
19. J.M. Delaye and D. Ghaleb, Proc. of. MRS Fall Meeting, Symposium on Glasses, Boston (1996).
20. S. Komarneni and M. Tsuji, J. Am. Ceram. Soc. 72, 1668 (1989).
21. I.G. Richardson, A.R. Brough, G.W. Groves, and C.M. Dobson, Cem. Concr. Res. 24, 813 (1994).